Methodological Details

Surgical procedures. A rhesus macaque (*Macaca mulatta*, female, 5 kg) was treated with two left intracarotid injections of MPTP to induce a moderate hemi-parkinsonian state (0.4-0.6 mg/kg per treatment). Pre-operative computed tomography (CT) and magnetic resonance imaging were performed and the resulting scans were co-registered in Analyze (Mayo Clinic). Anatomical reconstruction of the basal ganglia and placement of the cranial burr holes and cephalic chambers were determined using a custom software program (Miocinovic, et al., 2007) (**Fig. S1*A***). Chambers were positioned unilaterally along a coronal plane (DBS chamber) and a sagittal plane (motor cortex recording chamber) and were secured to the cranium with bone screws and dental acrylic. All procedures complied with the *NIH Guide for Care and Use of Laboratory Animals* and with the Cleveland Clinic Institutional Animal Care and Use Committee.

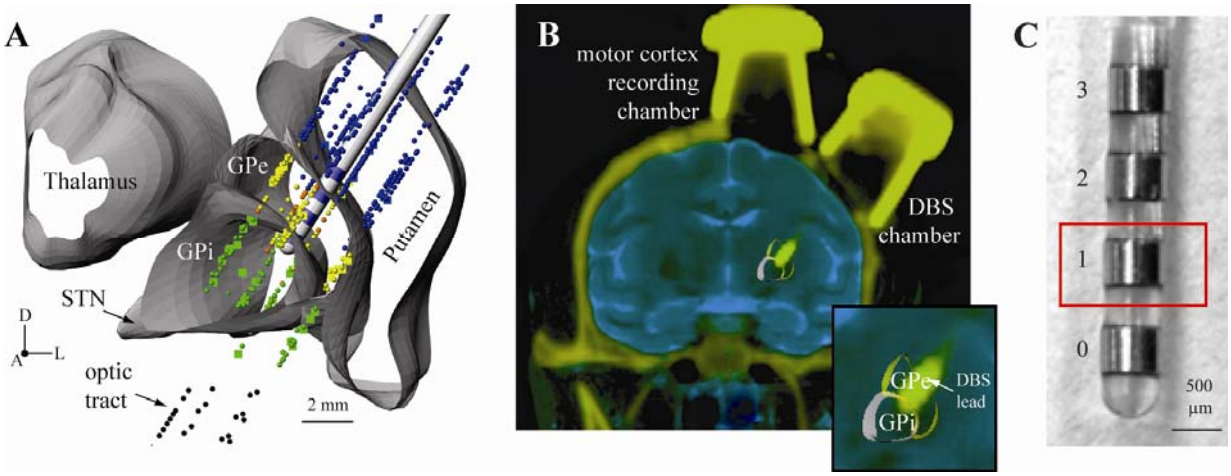

Figure S1: DBS lead localization in the MPTP-treated monkey. ***A,*** Initial boundaries of the globus pallidus were estimated using pre-operative magnetic resonance images and a 3D brain atlas. Borders of the pallidum and demarcations between pallidal segments were further constrained by identifying pallidal neurons during multiple microelectrode mapping sessions. ***B,*** Following DBS lead implantation, CT scans, MR images, and microelectrode recordings were used to determine the location of each electrode contact. ***C,*** The implanted lead consisted of four independent electrodes (contacts 0-3). Contact 1 was the electrode stimulated while performing microelectrode recordings in primary motor cortex.

Deep brain stimulation. After a recovery period, microelectrode penetrations were made through the coronal chamber to define anatomical boundaries of the pallidal segments prior to DBS lead implantation (**Fig. S1*A***). Neuronal activity was sampled at 25 kHz and filtered between 500-5000 Hz with an Alpha-Lab system (Alpha Omega). The external and internal segments of the globus pallidus (GPe and GPi) were identified by their

characteristic firing patterns in the parkinsonian state, and the sensorimotor territory within these nuclei were identified by their responses to sensorimotor stimuli (Filion, et al., 1988). Microstimulation (10-100 μA) was used to identify the corticospinal tract (CST) and recordings of evoked potentials to a strobe light were used to establish optic tract coordinates. The microelectrode track that yielded well-defined sensorimotor representations in both pallidal segments and high thresholds for CST fiber activation was chosen for the DBS lead implant. Following insertion of the lead to the target depth, the proximal end of the lead was secured with glue to an interlocking ring that fit within a cylindrical groove in the metal chamber (Elder, et al., 2005). Post-operative CT scans were co-registered with MRI scans to verify the final orientation and position of the DBS lead within the pallidum (**Fig. S1*B***). The implanted lead (Boston Scientific) was a scaled-version of a human DBS lead and consisted of four cylindrical contacts with heights of 500 μm, diameters of 750 μm, and inter-electrode spacing of 500 μm (**Fig. S1*C***). Lead wires from each of the contacts were connected to four channels of an externalized pulse generator (Itrel II, Medtronic). Stimulation was charge-balanced with parameters that varied in amplitude (0.5V, 1.0V, 1.5V, and 2.0V) and frequency (30 and 135Hz). The pulse width of the cathodic phase remained constant (90 μs).

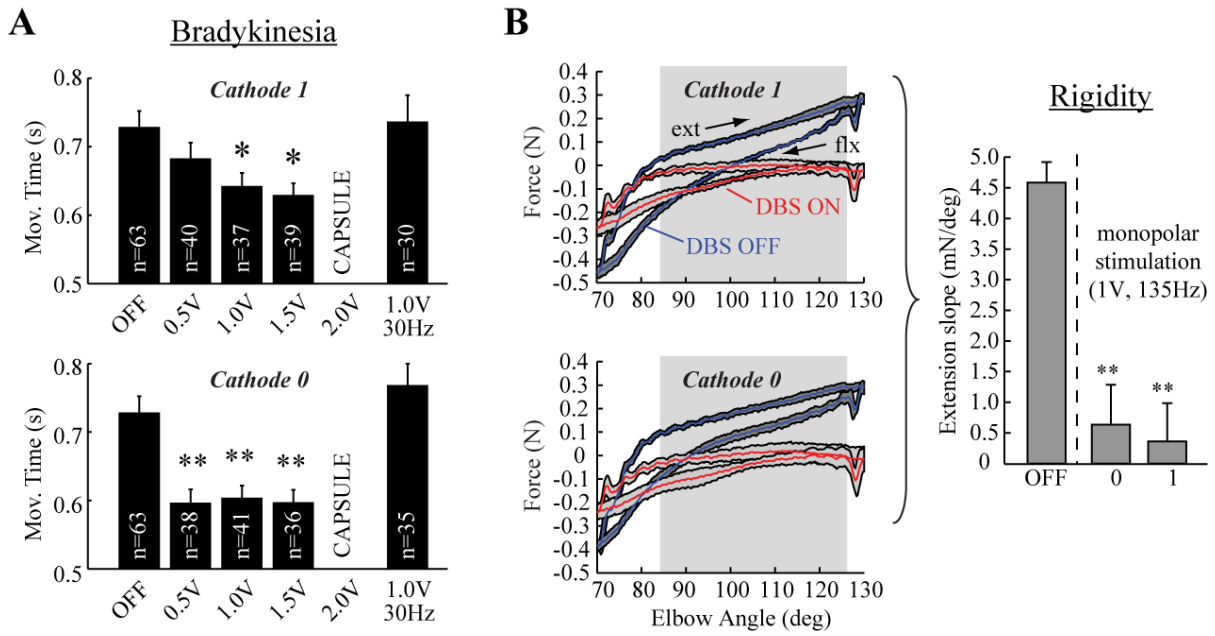

Figure S2: Stimulation settings that alleviated bradykinesia and rigidity were determined through a series of daily programming sessions. ***A,*** Monopolar DBS with the cathode as either 0 or 1 produced a significant reduction in movement time during the elbow extension and flexion phases of a reach and retrieval task for food reward. Cathode 1, in particular, exhibited two sub-therapeutic voltage settings (0.5V, 135Hz) and (1.0V, 135Hz). ***B,*** Elbow rigidity was evaluated quantitatively through a motorized force transducer system. Stimulation through either contact 0 or 1 (1V, 135Hz) generated a reduction in the force-angle slope during both extension and flexion phases. (ANOVA, **p<0.001, *p<0.05)

Behavioral analysis. Bradykinesia scores were calculated by having the monkey perform a reach and retrieval task for a fruit reward, recording the task on video at 30 frames/sec, and then quantifying the amount of time allocated to extension, grasping, and retrieval phases of the task. Randomized stimulation sessions were conducted over five days for each stimulation setting. Monopolar DBS (1V, 135Hz) with cathodes at contacts 0 or 1 produced significantly faster movements (**Fig. S2*A***). Muscle rigidity was assessed by extending and flexing the monkey's elbow joint with a motorized system and then recording the resistive forces to those movements with a force transducer (Mera, et al., 2009). Measurements were made before, during, and after DBS across all contacts to determine which stimulation settings improved rigidity (**Fig. S2*B***). DBS (1V, 135Hz) through either contact 0 or 1 yielded the most significant decrease in rigidity. Similar to the bradykinesia results, lowering the stimulation frequency or amplitude on contact 1 resulted in a sub-therapeutic outcome in arm rigidity (data not shown).

Microelectrode recording analysis. Tungsten microelectrodes with 0.6-1.2 MΩ impedances (FHC) were used to record single-unit activity in M1 (n=92 cells). Identification of M1 was verified by low threshold responses to microstimulation (10-30 μA, 400Hz, 200μs cathodic/anodic phase) and responsiveness to passive and active movement. Recordings were made with the monkey awake and sitting quietly in its chair while the experimenter passively manipulated the joint that resulted in firing rate changes in the recorded spike activity. Movement positions were digitized with a 3D motion capture system (Optotrak Certus, Northern Digital). Recordings in M1 were made before, during, and after DBS using contact 1 as the cathode and a cranial chamber as the return with stimulation settings that were either therapeutic (1V, 135Hz) or sub-therapeutic (0.5V, 135Hz and 1V, 30Hz) for rigidity and bradykinesia. Stimulation artifacts were removed from the recordings offline using a template-based subtraction method (Hashimoto, et al., 2003, Hashimoto, et al., 2002) (**Fig. S3**). Processed recordings were then discriminated and sorted offline (Offline Sorter, Plexon), and spike times were synchronized with the motion capture data (NeuroExplorer, NEX Technologies). Unit responses to passive movement were assessed with peri-event time histograms (PETH) (15-30 trials per unit, 10ms bin width). A discharge specificity ratio (DSR) was defined for each PETH as the averaged firing rate ratio between opposing joint articulations (for example, elbow extension versus elbow flexion). Peri-stimulus time histograms (PSTH) were generated for each unit (averaged over 30-90s, 0.1ms bin width), and responses during DBS were compared with those triggered to virtual stimulation epochs with

no DBS (**Fig. S3**). Histograms were smoothed with a 3-bin Gaussian filter. Population mean discharge rates and DSRs were compared between DBS ON and OFF states with paired t-tests (significance at $p<0.05$).

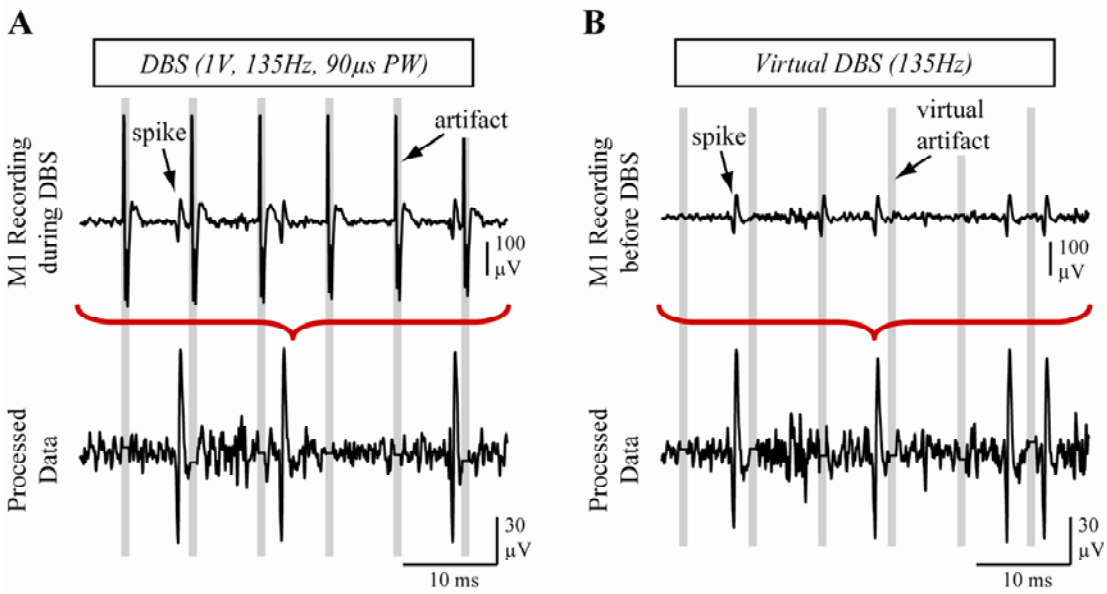

Figure S3. ***A,*** An automated offline algorithm generated templates of stimulation artifacts in the recording data sets and then subtracted those templates to uncover action potentials occurring between stimulus pulses (Hashimoto, et al., 2002). In general, 0.5-1.0 ms of recording data was deleted around each stimulation pulse. ***B,*** To prevent biasing the mean discharge rate during periods of no stimulation, a series of virtual stimulation epochs were introduced into the recordings with a frequency identical to that used during DBS. In this particular example, a virtual stimulation epoch overlapped with an action potential, which was hence removed from the processed recording stream. Note the different voltage-amplitude scales between the two rows.

References

1. Elder, C. M., Hashimoto, T., Zhang, J., and Vitek, J. L., 2005. Chronic implantation of deep brain stimulation leads in animal models of neurological disorders. J Neurosci Methods 142**,** 11-16.
2. Filion, M., Tremblay, L., and Bedard, P. J., 1988. Abnormal influences of passive limb movement on the activity of globus pallidus neurons in parkinsonian monkeys. Brain Res 444**,** 165-176.
3. Hashimoto, T., Elder, C. M., Okun, M. S., Patrick, S. K., and Vitek, J. L., 2003. Stimulation of the subthalamic nucleus changes the firing pattern of pallidal neurons. J Neurosci 23**,** 1916-1923.
4. Hashimoto, T., Elder, C. M., and Vitek, J. L., 2002. A template subtraction method for stimulus artifact removal in high-frequency deep brain stimulation. J Neurosci Methods 113**,** 181-186.
5. Mera, T. O., Johnson, M. D., Rothe, D., Zhang, J., Xu, W., Ghosh, D., Vitek, J., and Alberts, J. L., 2009. Objective quantification of arm rigidity in MPTP-treated primates. J Neurosci Methods 177**,** 20-29.
6. Miocinovic, S., Zhang, J., Xu, W., Russo, G. S., Vitek, J. L., and McIntyre, C. C., 2007. Stereotactic neurosurgical planning, recording, and visualization for deep brain stimulation in non-human primates. J Neurosci Methods 162**,** 32-41.